



Research Article

Exergoeconomic study of reheat combined cycle configurations using steam and ammonia-water mixture for bottoming cycle parameters

Mayank MAHESHWARI^{1,*}, Onkar SINGH²

¹Department of Mechanical Engineering, BBD University, Lucknow, 226028, India

²Department of Mechanical Engineering, Harcourt Butler Technical University, Kanpur, 208002, India

ARTICLE INFO

Article history

Received: 08 January 2022

Revised: 10 February 2022

Accepted: 11 February 2022

Keywords:

Exergy; Economics; Part Load Operations; Combined Cycle; Reheat Aqua Ammonia Turbine

ABSTRACT

The use of combined cycle power plants though had led the pathway to maximize the fuel energy utilization but the part-load operation of these plants is of concern. In this work, an exergoeconomic comparison of 11 different reheat combined cycle arrangements has been carried out under their part-load operations for varying bottoming cycle parameters namely steam-bleed fraction, deaerator pressure, separator temperature, absorber pressure, and condenser pressure. The results depict that the absorber has the highest exergy destruction with second law efficiency of 23.55% at the part load of 25% for the combined cycle power plant having high pressure drum with steam as working fluid and low pressure drum with ammonia-water as working fluid. The comparison also shows the highest cost of electricity production as 0.1243 USD/kWh for the combined cycle power plant having ammonia-water as working fluid in bottoming cycle and operating at part load of 25%. While the minimum price of electricity produced is 0.05 USD/kWh at 25% part load for CCPP having double pressure HRVG's at condenser pressure of 0.09 bar.

Cite this article as: Maheshwari M, Singh O. Exergoeconomic study of reheat combined cycle configurations using steam and ammonia-water mixture for bottoming cycle parameters. J Ther Eng 2023;9(5):1272–1290.

INTRODUCTION

In the recent past, the combined cycle power plants have become popular owing to their better performance due to an increase in available energy. Generally, the combined cycles have thermodynamic cycles operated synergetically for improving fuel energy utilization and there are numerous possibilities to maximize the available fuel energy utilization for cycle performance improvement. Along with the full load operation of the combined cycle power plant (CCPP),

its output and efficiency at part load operation are also of concern.

Exergoeconomic analysis is the tool that gives us the cost associated due to irreversibilities in various thermodynamic components of the power cycle, Tsatsaronis and Winhold [1]. Since a CCPP involves a huge cost so an overall approximate cost assessment of the plant and locating the sources of thermodynamic inefficiency in respective components can be done by exergoeconomic analysis, as

*Corresponding author.

*E-mail address: mayankmaheshwari80@rediffmail.com

This paper was recommended for publication in revised form by Regional Editor N. Filiz Özdi



per studies of Abusoglu and Kanoglu [2] and Tsatsaronis [3]. Among different methods of exergoeconomic analysis like SPECO, MOPSA, and Moran, the Moran method is simple as compared to the other two methods of exergy-based economic analysis. But the deviation in results produced with the Moran method is more as compared to the other two. Moreover, the Moran method applies to power plants when there is only one product of the power plant, Gorji-Bandpy and Ebrahimian [4]. Tsatsaronis et al. [5] suggested that the cost of irreversibility associated with the fluid should only be considered if it enters the thermodynamic system and that the cost should be removed when working fluid leaves the system. Zhang et al. [6] stated that for process systems, the sequential method for determining the cost of recoverable exergy is exergoeconomic losses. Ozdil, Tantekin and Pekdur [7] performed exergoeconomic analysis for a cogeneration plant of food industry and concluded that as steam pressure increases, the cost of unavailable energy increases for the boiler.

Various authors Balafkandeh [8] and Gholamian et al. [9] use the multi-objective optimization technique and exergoeconomic analysis to analyze the complex systems and identify the major sources of losses. Motamed and Nord [10] suggested the use of variable area nozzle to increase the part-load efficiency of the organic Rankine cycle. It is concluded that if the exhaust from the gas turbine is at constant temperature then part-load efficiency is better as compared to decreasing gas turbine exhaust temperature.

Özdil [11-13] and Tantekin [14] showed that available energy destruction is maximum where combustion of fuel takes place hence the cost of irreversibility is also highest where combustion takes place. Felleh et al. [15] and Yucer [16]. Li et al. [17] suggested the use of a back pressure turbine to decrease the part-load efficiency of combined cycle power plants. The authors concluded that with the use of a back pressure turbine the part-load efficiency improves by 1.67% with respect to the considered reference cycle. Moreover, with the use of back pressure turbine, the power distribution between the topping cycle and the bottoming cycle can also be adjusted. Liu et al. [18] proposed a partially recuperative gas turbine to reduce the part load losses and found that a maximum of 1.7% gain in efficiency was possible under off-design conditions but with a loss in power output. The effect of pressure variation was studied by authors Bakhshmand et al. [19], Sahin [20] Ameri, Ahmadi and Hamidi [21], and the findings indicate that the exergoeconomic losses reduce with an increase in pressure levels. Variny and Mierka [22] studied an 80 MW power plant for part-load operation for fuel savings and concluded that the controlling condensate preheating, changing steam condensing pressure, and gas turbine inlet air preheating, collectively can save the fuel by 2%.

The use of alternative fuels combined with conventional fuels may reduce the exergoeconomic loss of a power cycle but at the expense of the capital cost of the plant. But if a cycle is completely run on external-fired alternative fuel it may not be cost-effective, Soltani et al. [23]. Nevertheless, the use of supplementary firing leads to an increase in

power output of the cycle and also increases the cost of electricity produced as per the study of Khanmohammadi and Azimian [24]. The use of unconventional sources of energy may also reduce the losses occurring due to the part-load operation of CCPP, Mehrpooya Taromi and Ghorbani [25].

In a CCPP, HRSG forms a connecting thermodynamic element between the topping cycle and the bottoming cycle. The effect of the part-load operation on HRSG was studied by Najjar, Alaluland Abu-Shamleh [26]. The study observed that HRSG degradation increases if the part-load condition is maintained for a longer duration of time and the degradation was not affected by the ambient conditions. Moreover, the degradation in low-pressure HRSG was observed to be more in comparison to high-pressure HRSG under similar loading conditions. Jonshagen [27] suggested the use of stack gases from HRSG to increase the part-load efficiency of the combined cycle power plant. The study also suggested that the use of exhaust gas recirculation may impact in the maintenance period of the power plant.

As per Maheshwari and Singh, [28], turbine blade cooling had led the engineers to increase the turbine blade temperatures beyond their metallurgical limits. Song et al. [29] analyzed a GE-7F model of an air-cooled 150MW gas turbine and found that cooling of gas turbine affects the overall turbine efficiency.

The optimization techniques are useful in getting the intended objectives. Moreover, the use of the optimization technique can increase the first law and second law efficiencies, Ganjehkaviri et al. [30]. Liu and Karimi [31] proposed an optimal balance between the two techniques for part-load operations, fuel flow control, and the inlet guide vane control technique. This study suggested a multi-variable simulation-based optimization approach that maximizes the power cycle efficiency.

The use of genetic algorithm reduces the operational cost of ISCC by 11% and the cost of electricity produced by the steam turbine and gas turbine reduces by 7.1% and 1.7% respectively but at the expense of an increase in capital investment of the power plant by 13.3%. Baghernejad and Yaghoubi [32]. Lorencin et al [33] used genetic algorithm for electrical power output estimation. Dawo, Wieland and Spliethoff [34] analyzed a power plant based on binary mixture.

Research gap and problem formulation

Thus, the literature review presented demonstrates that the exergy-based economic analysis is used to determine the irreversibility associated with the cost for a given CCPP or CCHP with cooling. Literature also shows that the exergoeconomic analysis has been performed on the part-load operation of CCPP or CHP with cooling, and extended further to the cooled gas turbine model. Thus, it is evident that although work is done on exergy based economic analysis of plant for its part-load operation but the following need to be studied:-

- Effect of binary fluid as-
 - (i) Working fluid in bottoming cycle
 - (ii) As closed-loop coolant to gas turbine blades
- Effect of bottoming cycle parameters

Because of the above, the objective of the present work involves, the determination of second law efficiency and the

with the provision of reheating of expanding gases in the reheat combustion chamber placed in between the two turbines. Thereafter expanding flue gases enter the HRSG/HRVG, where bottoming cycle working fluids (i.e., either water or ammonia-water mixture or both) are heated and converted to their respective vapor form.

Work is extracted from bottoming cycle at different pressure levels (either from double or triple pressure HRSG/HRVG) due to the expansion of working fluid i.e. steam or

binary mixture. After expansion in bottoming cycle, the working fluid goes to the condenser and then to HRSG/HRVG. Part of working fluid act gas turbine blades coolant.

The CCPP configurations depicted from Figure 2 – Figure 12 possess the following major features in their layouts

- Figure 2 is a cycle having triple pressure HRSG with cooled blades of turbo machine using steam only.

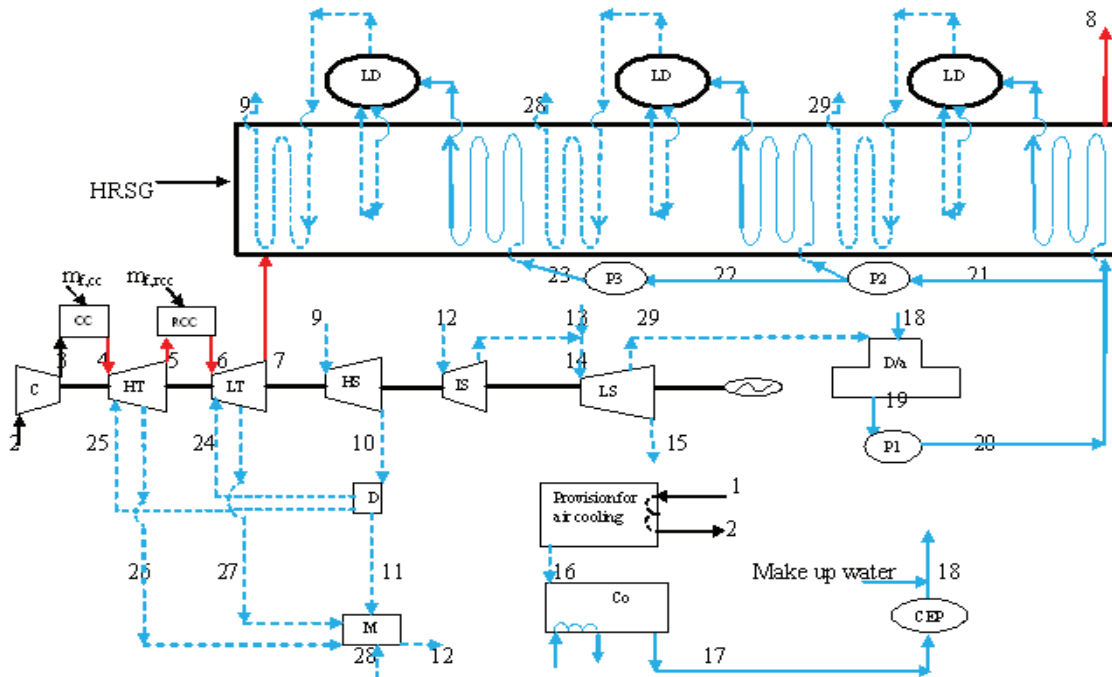


Figure 2. Combined reheat type steam cooled topping cycle with steam bottoming cycle (RGSSC).

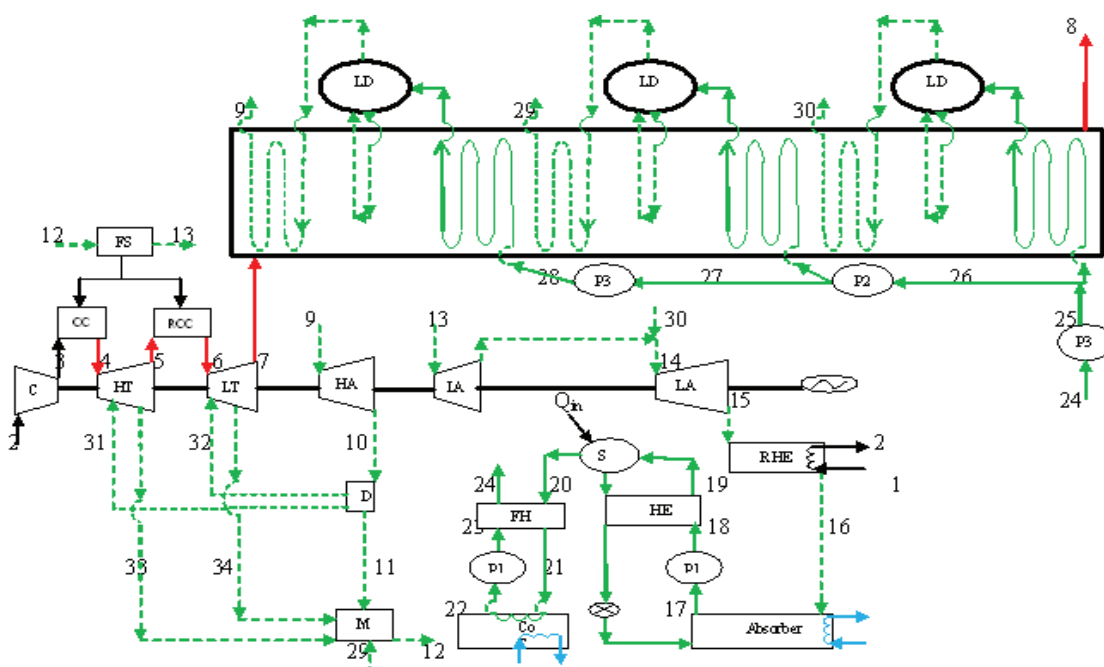


Figure 3. Combined reheat type aqua ammonia cooled topping cycle with aqua ammonia bottoming cycle (RGAAC).

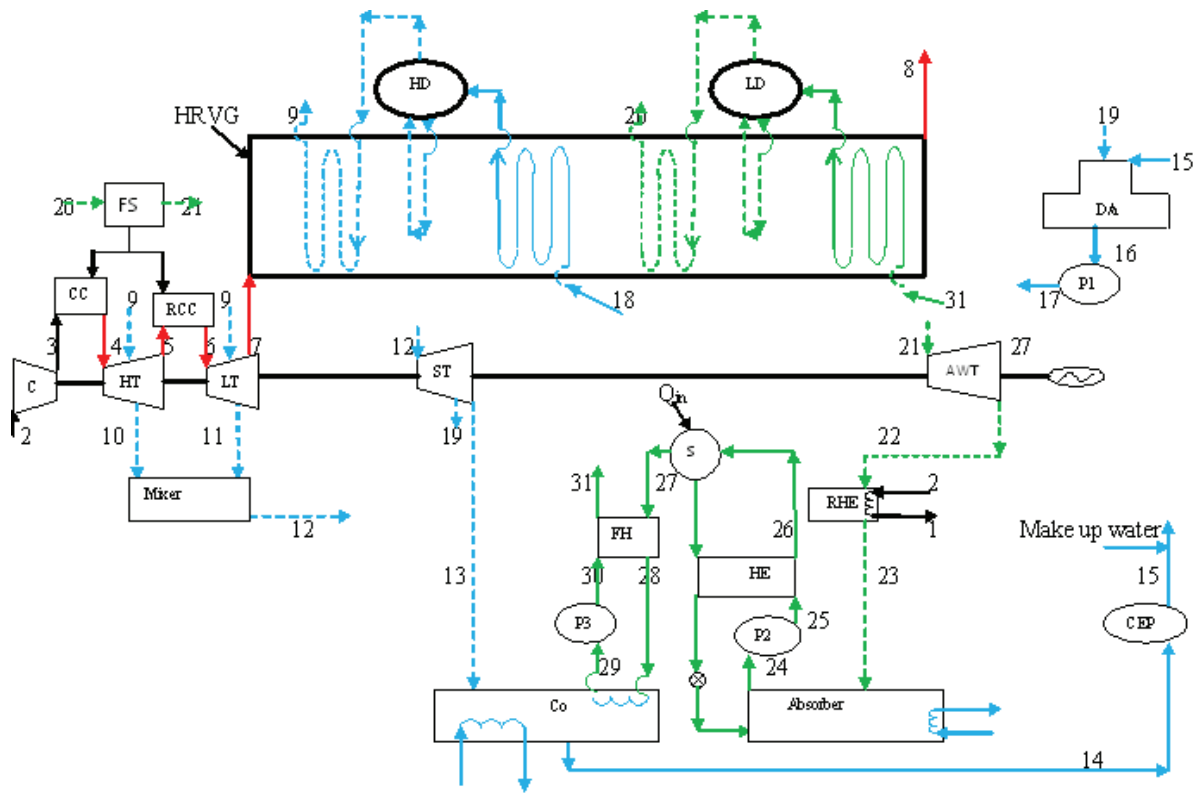


Figure 4. Combined reheat type steam cooled topping cycle with steam and aqua ammonia bottoming cycle (RGSASC).

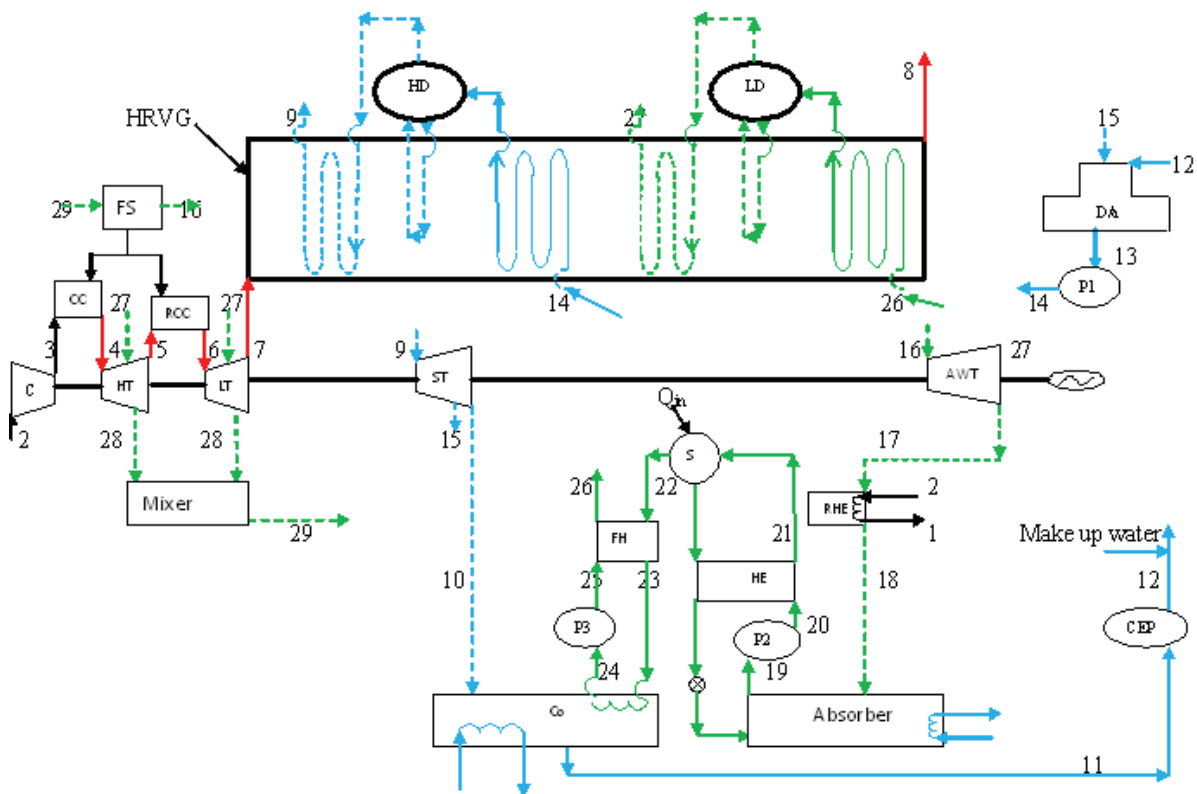


Figure 5. Combined reheat type aqua ammonia cooled topping cycle with steam and aqua ammonia bottoming cycle (RGSAAAC).

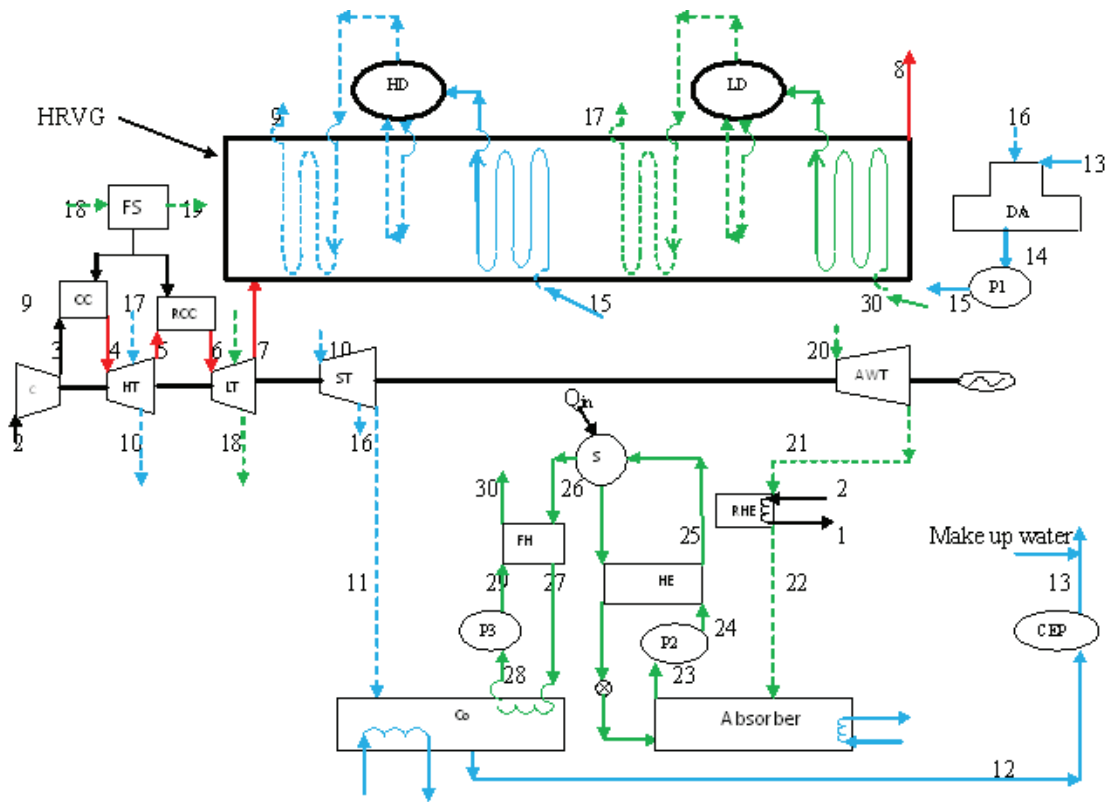


Figure 6. Combined reheat type steam and aqua ammonia mixture cooled topping cycle with steam and aqua ammonia bottoming cycle (RGSASAC).

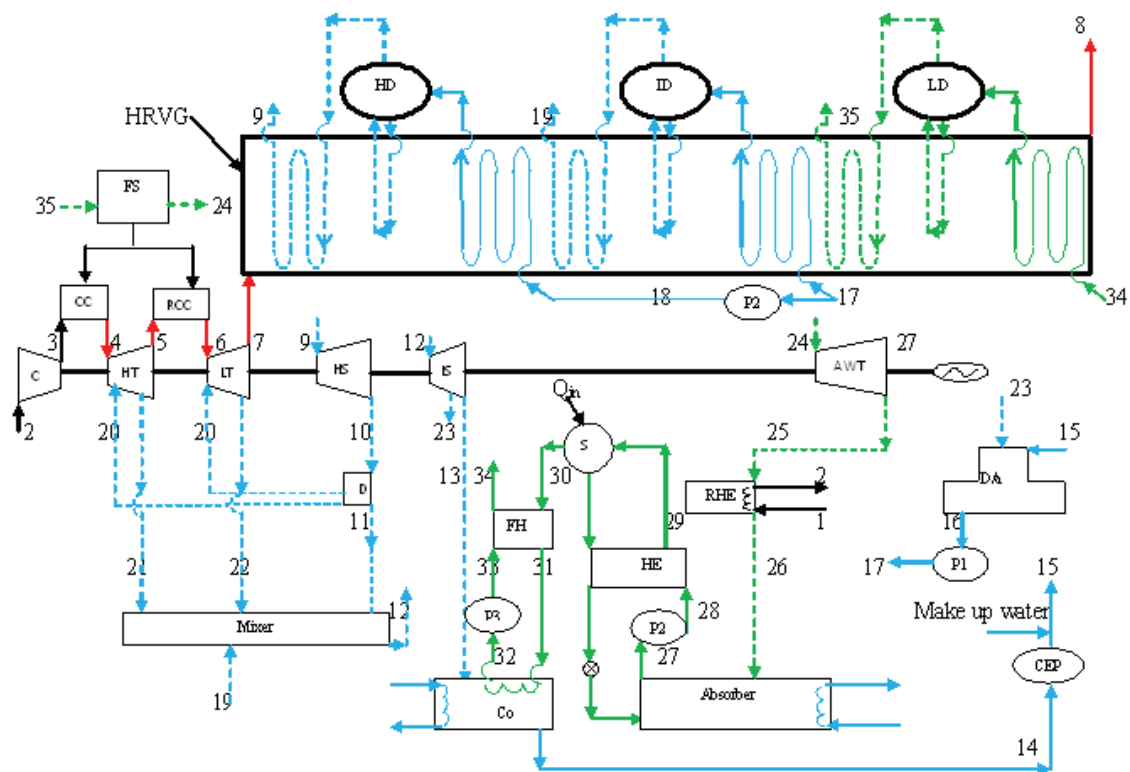


Figure 7. Combined reheat type steam cooled topping cycle with reheat steam and aqua ammonia bottoming cycle (RGRSASC).

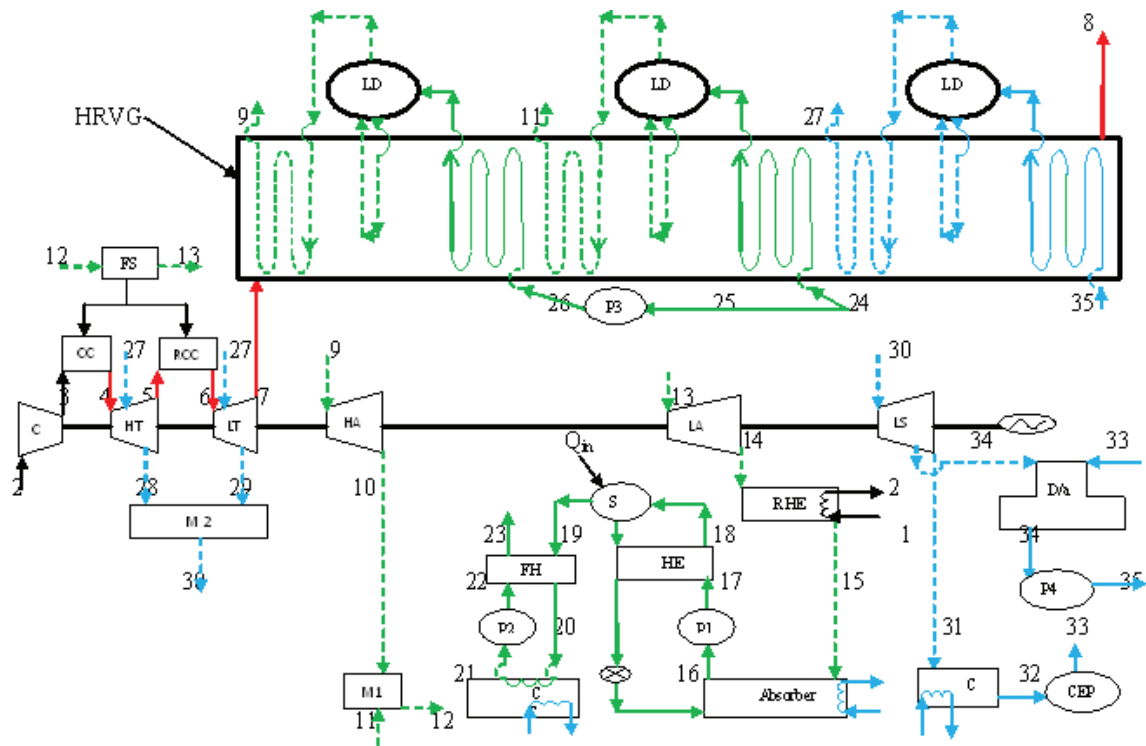


Figure 10. Combined reheat type steam cooled topping cycle with steam and reheat aqua ammonia bottoming cycle (RGRASC).

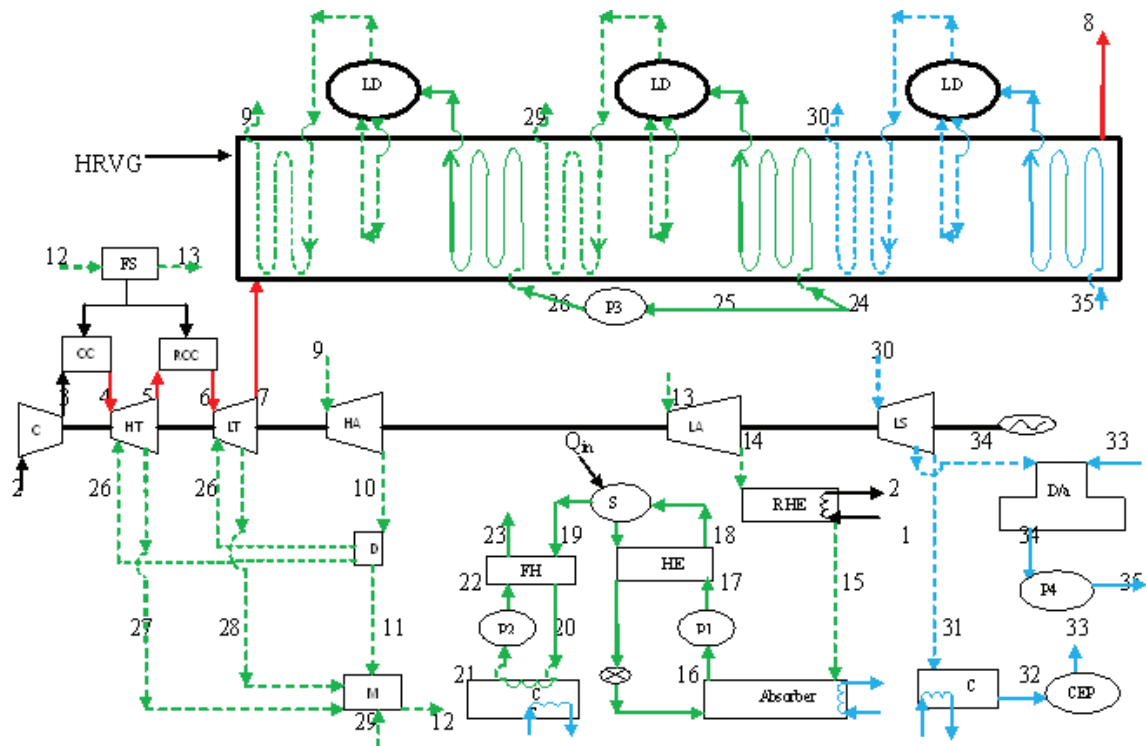


Figure 11. Combined reheat type aqua ammonia mixture cooled topping cycle with steam and reheat aqua ammonia bottoming cycle (RGSRAAC).

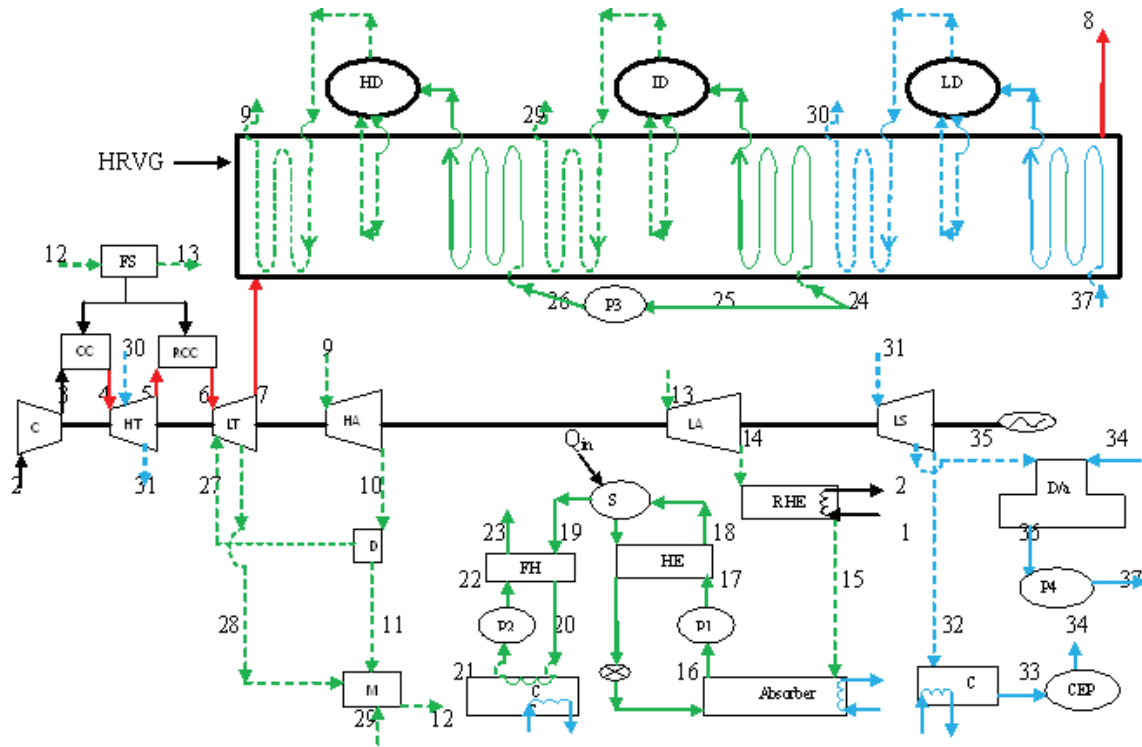


Figure 12. Combined reheat type steam and aqua ammonia mixture cooled topping cycle with steam and reheat aqua ammonia bottoming cycle (RGSRASAC).

- Figure 3 is a cycle having triple pressure HRVG with cooled blades of turbo machine using binary fluids only.
- Figure 4- Figure 6 are cycles having double pressure HRVG with variation in turbo machine blade cooling technique.
- Figure 7- Figure 12 are CCPP with tri-generation in bottoming cycle along with variation in turbo machine blade cooling technique.

Methodology:

Following major assumptions are made in the analyses of the present study:

- During part-load operations, there is no change in the parameters of thermodynamic components.
- Concentration of ammonia is taken to be 0.7 in the analyses, Maheshwari and Singh [41].
- Specific exergy costing methodology is used for evaluating the performance of various thermodynamic components.

The cost balance equation for the k^{th} component can be written as

$$\sum \dot{C}_{out,k} + \dot{C}_{w,k} = \sum \dot{C}_{in,k} + \dot{C}_{q,k} + \dot{Z}_k \quad (1)$$

Where

$$\dot{Z}_k = \dot{Z}_k^{CI} + \dot{Z}_k^{OM} \quad (2)$$

$$\dot{C}_{in} = c_{in} \dot{E}_{in} \quad (3)$$

$$\dot{C}_{out} = c_{out} \dot{E}_{out} \quad (4)$$

$$\dot{C}_q = c_q \dot{E}_q \quad (5)$$

$$\dot{C}_w = c_w \dot{W} \quad (6)$$

$$\dot{Z}_k^{CI} = \left[\frac{CRF}{n} \right] \cdot Z_k \quad (7)$$

$$CRF = \frac{i_r(1+i_r)^n}{(1+i_r)^n - 1} \quad (8)$$

Thus, the second law efficiency of combined cycle can be written as

$$\eta_{II,combined\ cycle} = \frac{W_{combined\ cycle} + Q_{cool}}{\dot{m}_f \cdot G_r} \quad (9)$$

The thermodynamic modeling and cost estimations for the constituent components of the arrangements are taken from the works of Prakash and Singh [42], Singh and Singh [43] Owebor et al. [44], Campbell [45], Gülen [46], CERC [47] detailed in Table 1.

Table 1. Irreversibility and the associated cost function of different thermodynamic components

Component	Irreversibility associated with component	Cost function
Compressor	$\dot{I}_{\text{compressor}} = T_o \cdot [\dot{m}_a \cdot (s_{a,e} - s_{a,i})]$	$C_c = \frac{39.5 \cdot (\dot{m}_a)}{0.9 - \eta_c} \left(\frac{P_{e,c}}{P_{i,c}} \right) \ln \left(\frac{P_{e,c}}{P_{i,c}} \right)$
Combustion Chamber	$\dot{I}_{\text{cc}} = T_o \cdot [\dot{m}_{\text{fg}} \cdot s_{\text{fg}} - \dot{m}_{a,i} \cdot s_{a,i}]$	$C_{\text{cc}} = \frac{46.08 \cdot \dot{m}_f}{0.995 - \left(\frac{P_{e,cc}}{P_{i,cc}} \right)} [1 + \exp(0.018 \cdot T_{e,cc} - 26.4)]$
Gas turbine	$\dot{I}_{\text{gt}} = T_o \cdot [\dot{m}_{\text{fg}} \cdot (s_{\text{fg},i} - s_{\text{fg},e}) + \sum_{\text{stage}} \dot{m}_{\text{coolant}} \cdot (s_{\text{coolant},e} - s_{\text{coolant},i})]$	$C_{\text{gt}} = W_{\text{gt}} [1318.5 - 98.328 \cdot (\ln W_{\text{gt}})]$
Bottoming cycle turbine	$\dot{I}_{\text{st/amwt}} = T_o \cdot [\dot{m}_{\text{st/amwt}} \cdot (s_{\text{st/amwt},i} - s_{\text{st/amwt},e})]$	$C_{\text{st/amwt}} = 6000 \cdot (W_{\text{st}} + W_{\text{amwt}})^{0.7}$
Pump	$\dot{I}_{\text{pump}} = T_o [\dot{m}_{\text{st/amwt}} (s_o - s_i)]$	$C_{\text{pump}} = 705.48 \cdot (W_{\text{pump}})^{0.71} \cdot \left(1 + \frac{0.2}{1 - \eta_{\text{pump}}} \right)$
Condenser	$\dot{I}_{\text{condenser}} = T_o \left[\sum_j \dot{m}_j \cdot (s_{j,i} - s_{j,o}) - m_w c_{p,w} \ln \frac{T_{w/i}}{T_{w/o}} \right]$	$C_{\text{s/amw}} = 1773 \cdot \dot{m}_w$
Mechanical chiller	$\dot{I}_{\text{M/C}} = T_o \cdot [\dot{m}_a \cdot (s_{a,i} - s_{a,o})]$	$C_{\text{M/C}} = 4745 \cdot \left(\frac{\dot{Q}_{\text{M/C}}}{\log \Delta T_{\text{M/C}}} \right)^{0.8} + 11820 \cdot (\dot{m}_s + \dot{m}_a)$
Heat exchanger	$\dot{I}_{\text{HE}} = T_o [m_{\text{we/sol}} \cdot (s_{\text{we/sol},i} - s_{\text{we/sol},o}) - m_{\text{w/sol}} \cdot (s_{\text{w/sol},o} - s_{\text{w/sol},i})]$	$C_{\text{HE}} = 4745 \cdot \left(\frac{\dot{Q}_{\text{M/C}}}{\log \Delta T_{\text{M/C}}} \right)^{0.8} + 23640 \cdot \dot{m}_{\text{amw}}$
Refrigerant heat exchanger	$\dot{I}_{\text{RHE}} = T_o \cdot [\dot{m}_{\text{amw}} \cdot (s_{\text{amw},o} - s_{\text{amw},i}) - \dot{m}_{\text{air}} \cdot (s_{a,o} - s_{a,i})]$	$C_{\text{RHE}} = 4745 \cdot \left(\frac{\dot{Q}_{\text{RHE}}}{\log \Delta T_{\text{RHE}}} \right)^{0.8} + 11820 \cdot (\dot{m}_{\text{amw}} + \dot{m}_a)$
Feed heater	$\dot{I}_{\text{FH}} = (s_{\text{r/sol},i} - s_{\text{r/sol},o}) - (s_{\text{fr/sol},o} - s_{\text{fr/sol},i})$	$C_{\text{FH}} = 4745 \cdot \left(\frac{\dot{Q}_{\text{FH}}}{\log \Delta T_{\text{FH}}} \right)^{0.8} + 23640 \cdot \dot{m}_{\text{amw}}$
Absorber	$\dot{I}_{\text{Absorber}} = T_o \left[\dot{m}_{\text{wo/sol}} \cdot (s_{\text{mix},i} - s_{\text{mix},o}) - m_w c_{p,w} \ln \frac{T_{w/i}}{T_{w/o}} \right]$	$C_{\text{Absorber}} = 130 \cdot \left(\frac{A_{\text{abs.}}}{0.093} \right)^{0.78}$
Deaerator	$\dot{I}_{\text{D/a}} = T_o \cdot [\dot{m}_{\text{d/a,w}} \cdot s_{\text{d/a,w}} - \dot{m}_{\text{w,i}} \cdot s_{\text{w,i}} - \dot{m}_{\text{b/s,i}} \cdot s_{\text{b/s,i}}]$	$C_{\text{D/a}} = 4745 \cdot \left(\frac{\dot{Q}_{\text{D/a}}}{\log \Delta T_{\text{D/a}}} \right)^{0.8} + 11820 \cdot (\dot{m}_s + \dot{m}_{\text{amw}})$
Fuel Compressor	$\dot{I}_{\text{compressor}} = T_o \cdot [\dot{m}_f \cdot (s_e - s_i)]$	$C_{\text{fc}} = \frac{39.5 \cdot \dot{m}_f}{0.9 - \eta_c} \left(\frac{P_{e,fc}}{P_{i,fc}} \right) \ln \left(\frac{P_{e,fc}}{P_{i,fc}} \right)$
HRSG/HRVG	$\dot{I}_{\text{HRSG}} = T_o \cdot \left[\sum_j \dot{m}_j \cdot (s_{j,i,\text{HRSG/HRVG}} - s_{j,o,\text{HRSG/HRVG}}) - \frac{\dot{m}_{\text{fg}}}{M_{\text{fg}}} \left[\bar{c}_{p,\text{fg},i}^s \ln \frac{T_{\text{fg},i}}{T_o} - \bar{c}_{p,\text{fg},o}^s \ln \frac{T_{\text{fg},o}}{T_o} \right] + R_{\text{fg}} \cdot \left(\frac{\Delta p}{p_a} \right) \right]$	$C_{\text{HRSG/HRVG}} = 4745 \cdot \left(\frac{\dot{Q}_{\text{HRSG/HRVG}}}{\log \Delta T_{\text{HRSG/HRVG}}} \right)^{0.8} + 11820 \cdot (\dot{m}_s + \dot{m}_{\text{amw}}) + 658 \cdot \dot{m}_{\text{fg}}$
Fuel Preheater	$\dot{I}_{\text{fp}} = T_o \cdot [\dot{m}_{f,i} \cdot s_{f,i} - \dot{m}_{f,e} \cdot s_{f,e}]$	$130 \cdot \left(\frac{A_{\text{fp}}}{0.093} \right)^{0.78}$

Table 1. Irreversibility and the associated cost function of different thermodynamic components

Component	Irreversibility associated with component	Cost function
Value (in terms of monetary) of electricity generated	$\frac{\omega}{Po} \cdot \frac{\alpha}{T} + \frac{\gamma}{\eta} + \left[\frac{FIX}{Po \cdot T} + y \cdot VAR \right]$ Where $\omega = \left[\frac{(1+d_e)^t - 1}{(1+d_e)^n \cdot d_e} \right] \left[\frac{(1+x)^t \cdot x}{(1+x)^n - 1} \right]$ and $\gamma = \omega \cdot (FIX + VAR)$, VAR = Cost of fuel+ Cost of Ammonia-water mixture	
Other parameters	Rate of concession in % (x) = 10 Total design life considered for the power plant in years (t) = 10 Total operational time of power plant per year (T) = 8000 hours de = 4% Maintenance cost including risk factors (y) = 2.5	

Table 2. Input parameters considered for analysis [Sanjay [35], Zare [36], Yari [37], Yari [38]]

Component	Value
Topping cycle parameters	Polytropic efficiency of topping cycle turbo machines, (η_{tc}) = 92.0 % Combustor efficiency, (η_{cc}) = 99.5% Pressure loss in combustor , (p_{loss}) = 2% of p_i Heating value of fuel when water is assumed to be in vapour state after combustion = 48990 kJ/kg Stack gases pressure = 1.08 bar $T_b = 1123$ K
HRSG /HRVG	Effectiveness of heat exchanging element= 98.0 % Loss in pressure in heat exchangers= 10% of entry pressure (for both fluids) Range of pressure in the drums =4-160 bar (max.) Minimum stack gases temperature = 353.0 K Approach pointand Pinch point= 20.0 K (min.)
Bottoming cycle parameters	Maximum temperature at inlet to bottoming cycle turbine(s) = 873K Isentropic efficiency of bottoming cycle turbines, ($\eta_{is, hp}$) = 88.0 % Quality of steam at inlet to condenser = 0.85 (min.) Exhaust pressure from bottoming cycle turbine = 0.07 bar (min.) D/a = 2.0 bar Isentropic efficiency of pump's, (η_{pump}) = 88.0 %
Dead State	$P_o = 1.01325$ bar, $T_o = 298$ K

Table 2 depicts the base parameters considered for analysis along with the details of related references.

RESULTS AND DISCUSSION

The methodology developed under section 2.2, gives the following results which are discussed ahead.

Variation in electricity cost and second law efficiency for varying steam bleed fractions is shown in Figure 13. The graph depicts that for given steam bleed fraction and fix part load, the second law efficiency is minimum for double pressure HRSG/HRVG. This may be because the steam

bleed temperature is higher for the case of double pressure HRSG/HRVG as compared to triple ressure.

Figure 13. Variation in electricity cost and second law efficiency for varying steam bleed fractions.

Thus, the stream of high temperature working fluid increases the irreversibility in the form of

- Loss in work output (or available energy)
- Mixing of high temperature fluid in deaerator.

For the given configuration and part load, the increase in steam bleed fraction leads to a decrease in the second law efficiency because of the increase in the mass of working fluid taken out for deaeration purposes. Thus, the destruction of available energy increases hence second law

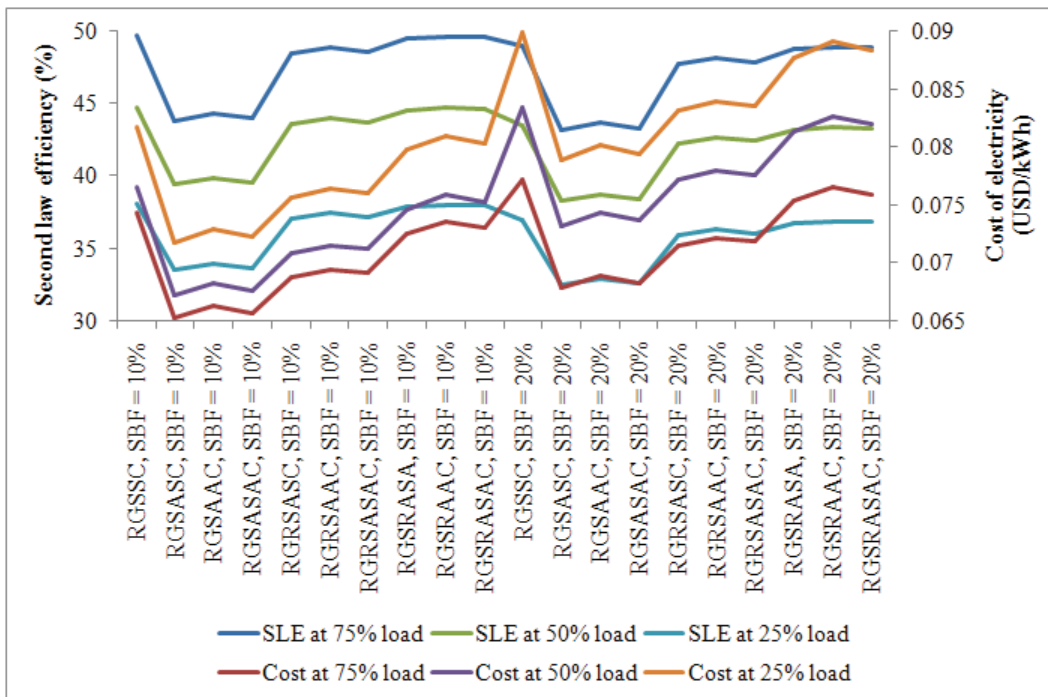


Figure 13. Variation in electricity cost and second law efficiency for varying steam bleed fractions.

efficiency decreases. Figure 13 also shows that if the part-load decreases then the second law efficiency decreases because of lesser work output obtained for the same turbine inlet temperature.

The effect of deaerator pressure on the cost of electricity and second law efficiency for different reheat cycle configurations is shown in Figure 14. For fixed loading conditions the graph depicts that as the deaerator pressure increases, the second law efficiency decreases because more

useful energy which can be converted into work is extracted out for deaeration purposes, thus a loss in work output. Moreover, this extracted stream of steam mixes with feed water, hence increasing the irreversibility. Thus, there is a loss of available energy in the form of work and the mixing of streams.

The increase in separator temperature depicts a loss of availability for all the configurations and hence an increase in the cost of electricity production as shown in Figure 15.

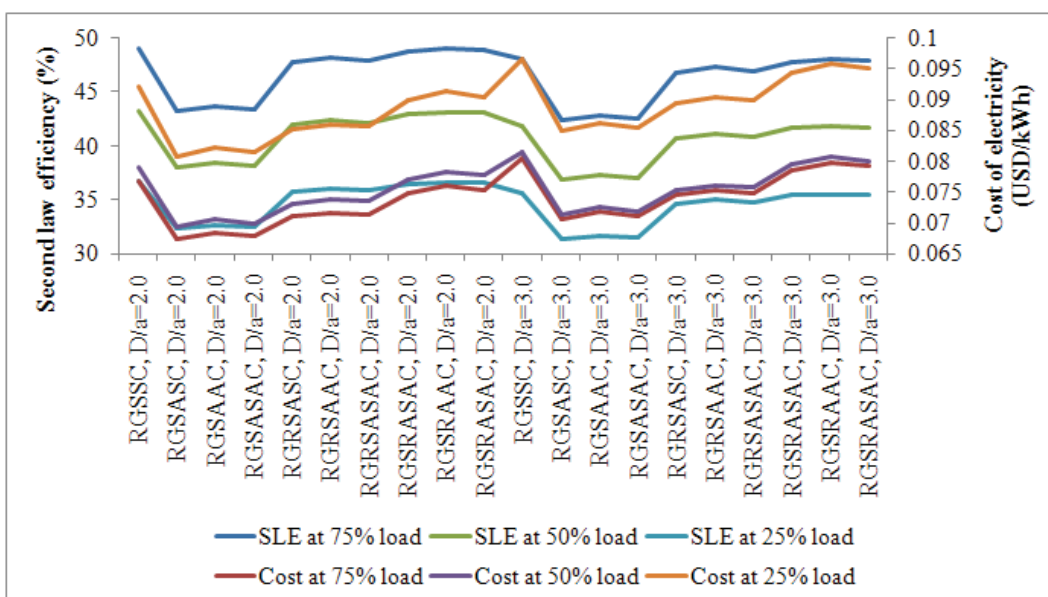


Figure 14. Variation in electricity cost and second law efficiency for varying deaerator pressure.

The exergy loss is because of the increased fuel consumption i.e., more available energy which is not utilized for any useful work.

Figure 15 depicts that for a constant separator temperature, as the pressure level of bottoming cycle increases (i.e., from double generation to triple-generation cycle) work output, electricity cost and the second law efficiency also increases.

As the absorber pressure is increased, the irreversibility due to mixing increases, shaft work of the binary mixture turbine reduces, Figure 16 These two factors results in reduction in second law efficiency of all the configurations. Although the cost of electricity produced decreases with an increase in absorber pressure. It is evident that as the load on the CCPP is reduced the cost of electricity for all the configurations gets increased as shown in the figure.

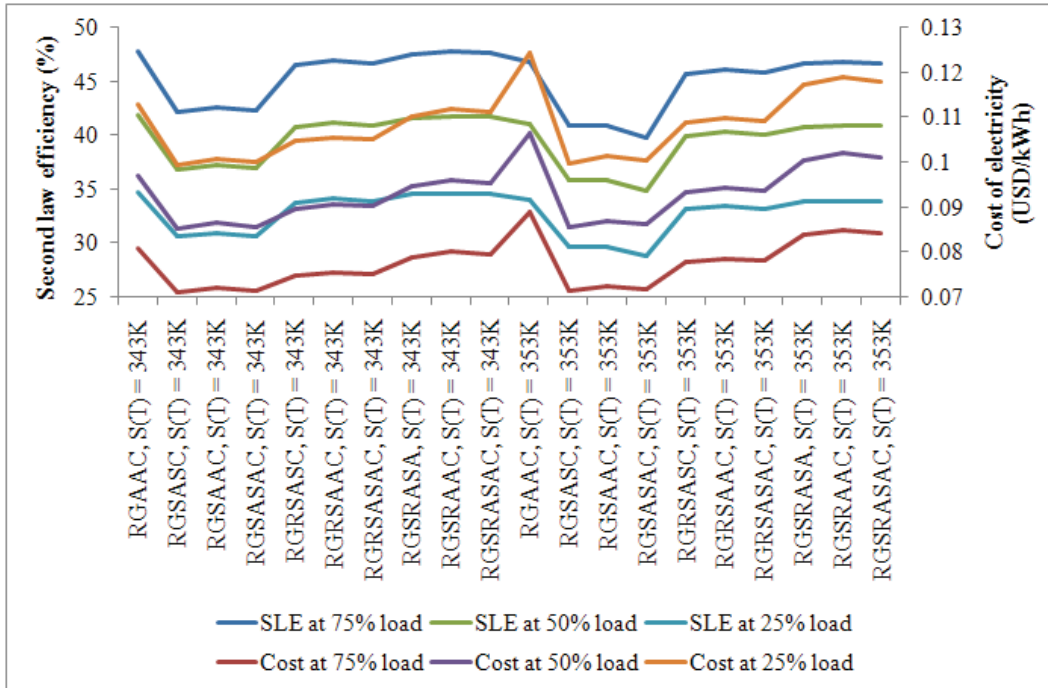


Figure 15. Variation in electricity cost and second law efficiency for varying separator temperature.

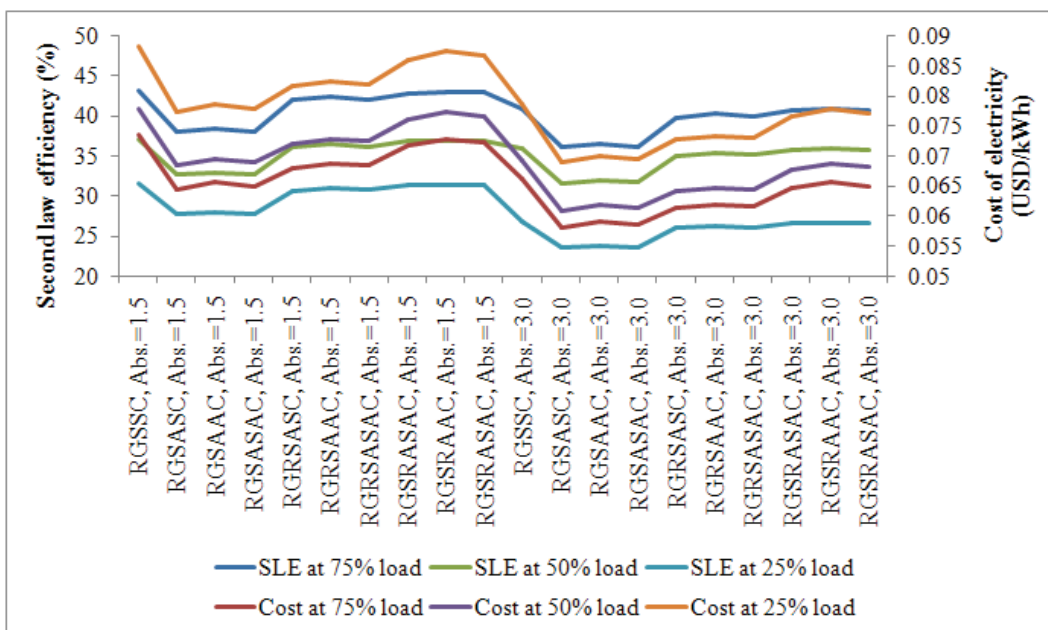


Figure 16. Variation in electricity cost and second law efficiency for varying absorber pressure.

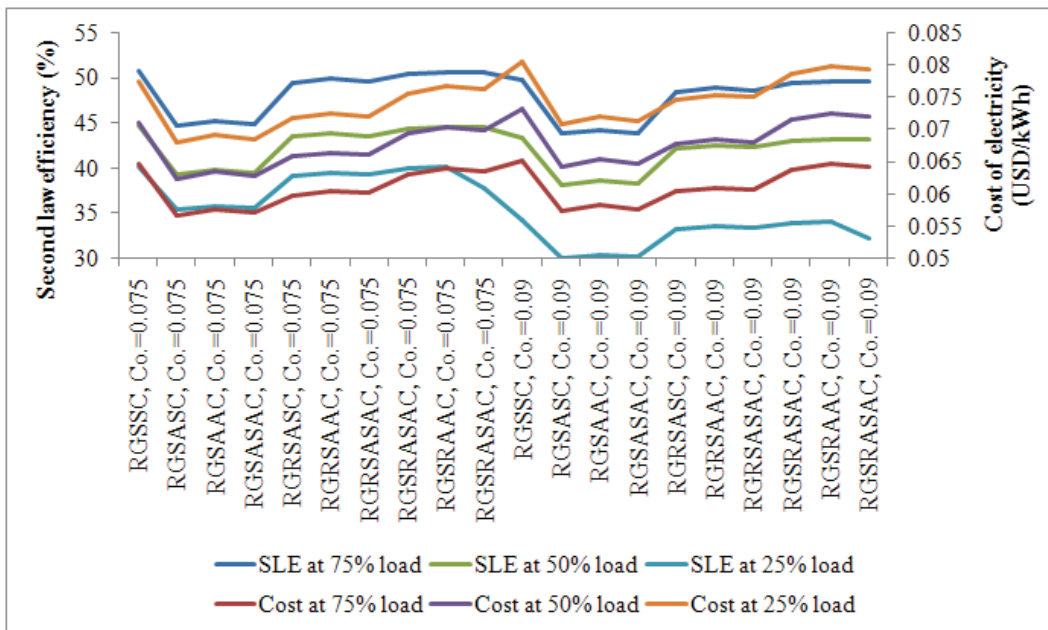


Figure 17. Variation in electricity cost and second law efficiency for varying condenser pressure.

Figure 17 depicts the variation of cost of electricity with condenser pressure. The graph follows the same pattern as that of absorber but with reduced intensity. This is because the mixing of fluids does not take place in the condenser and hence the irreversibility is less as compared to the absorber.

Effect on cost of electricity production:

Though the topping cycle configurations are similar for each configuration, still the cost of electricity produced varies for each configuration. This variation in cost may be due to bottoming cycle variants or their process parameters as detailed ahead.

Fixed and maintenance cost - As the number of thermodynamic components associated with the power generation cycle increases, its cost increases. Thus, the maintenance cost of the triple pressure cycle will be more as compared to double pressure and so on. Therefore, the discussion on the cost of electricity produced is limited to the configurations namely, RGSSC, RGRSASC, RGRSAAAC, RGRSASAC, RGRSRASC, RGSRAAC, and RGRSRASAC with the following considerations.

- As regards, the choice of the working fluid, the water is available in abundance at no cost, but there is a fixed cost associated with the ammonia-water mixture. So, as the number of components associated with the ammonia-water mixture increases, the cost of the plant increases.
- The use of binary mixture is done as a fuel preheater in the combustion chamber.

The analysis of the cost of electricity produced due to variation of steam bleed, Figure 13 for SBF = 10% at 75% of full load yields that among the aforesaid configurations

RGSSC shows the highest cost of electricity production followed by RGRSRASAC. RGSSC is a tri-generation cycle hence loss of available energy is more in it as compared to RGRSRASAC because the ammonia-water mixture offers better matching of temperature profiles and thus, more available energy for producing work. Also, there will be a loss of available energy in HRSG, mechanical chiller, and mixing of steam in the mixer in RGSSC, thereby increasing the electricity cost of production.

Same pattern is observed for 20% of steam bleeding as that of SBF = 10% and the same discussion holds good for deaerator pressure of 2.0 bar as shown in Figure 14.

In Figure 15, as the separator temperature is increased from 343K to 353K, the configuration RGAAC depicts the highest cost of electricity produced, because of the additional heat input which is given to the separator in the form of fuel.

The graphical results of Figure 16 and Figure 17 depict that electricity cost is maximum for the RGAAC when absorber pressure is considered and for the RGRSRASAC when condenser pressure is considered, because of the available energy being destroyed in absorber and condenser. This destruction of available energy increases as the part loading increases.

Figure 18 depicts the exergy destroyed in various components of layout RGSRAAC for a given set of condition -

- Part load of 77%, Steam bleed fraction of 10%,
- Deaerator pressure of 2.0 bar, Separator temperature of 343K.
- Absorber pressure of 1.5 bar and Condenser pressure of 0.075 bar.

Figure 18 demonstrates that available energy destruction shares a larger percentage where combustion of the fuel takes place. But the summation of exergy destroyed in waste heat recovery heat exchanger, absorber, and feed heater is comparable to the exergy destroyed in the combustion chamber

Figure 18 E-Sankey diagram for the exergy destruction along with the cost associated in different components of RGSRAAC.

Taking the available energy of fuel at the input to the combustion chamber as \$0.2kJ/kg, Dawo et al. [34], the cost of exergy destroyed in various components is indicated in Figure 18. These costs are determined based on exergy destroyed in respective components concerning the cost of fuel at the inlet to the combustion chamber.

Figure 19 compares the work of Yucer [16] with the modeling done in the present work on the basis of exergy efficiency of components, which is given by

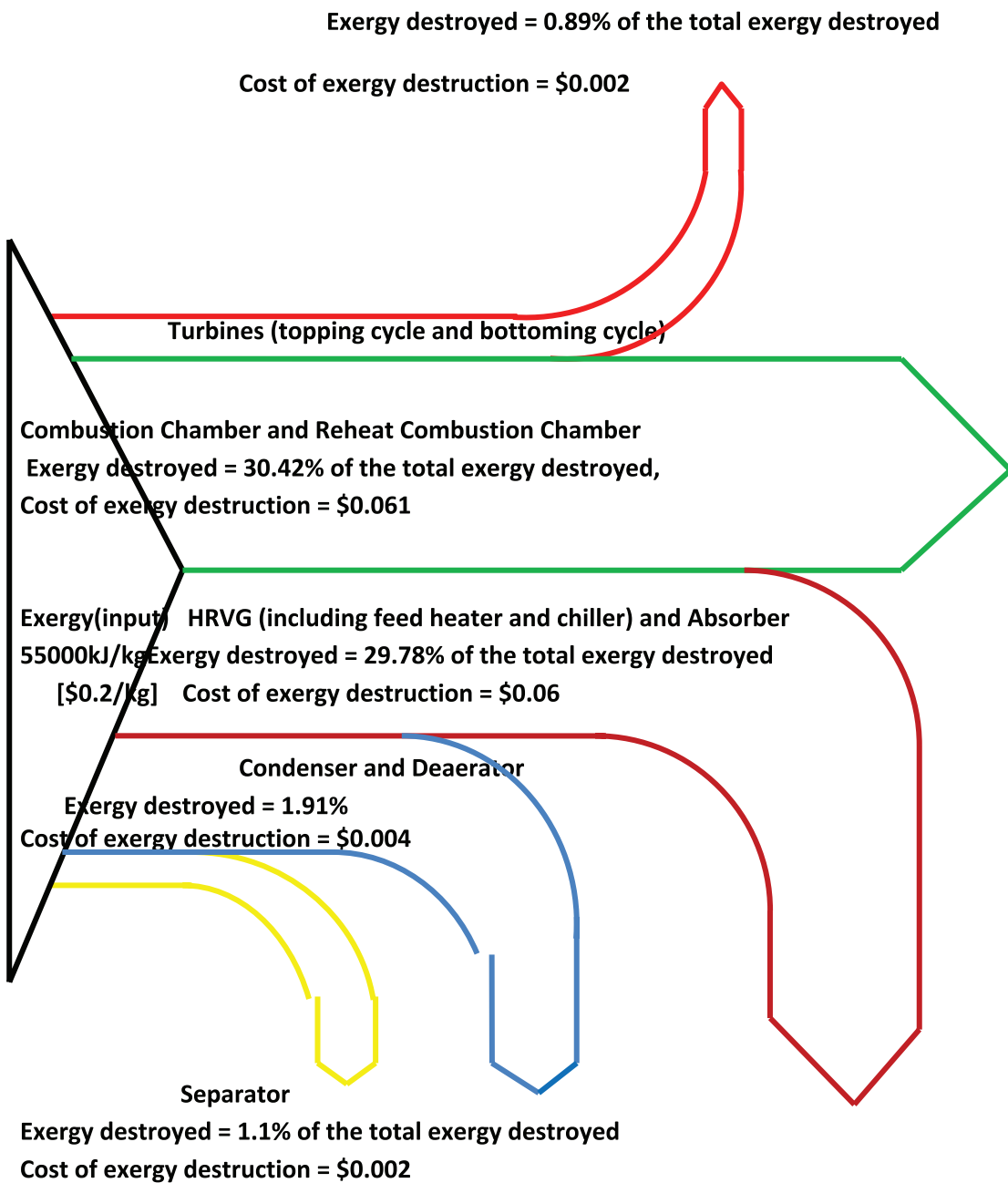


Figure 18. E-Sankey diagram for the exergy destruction along with the cost associated in different components of RGS-RAAC.

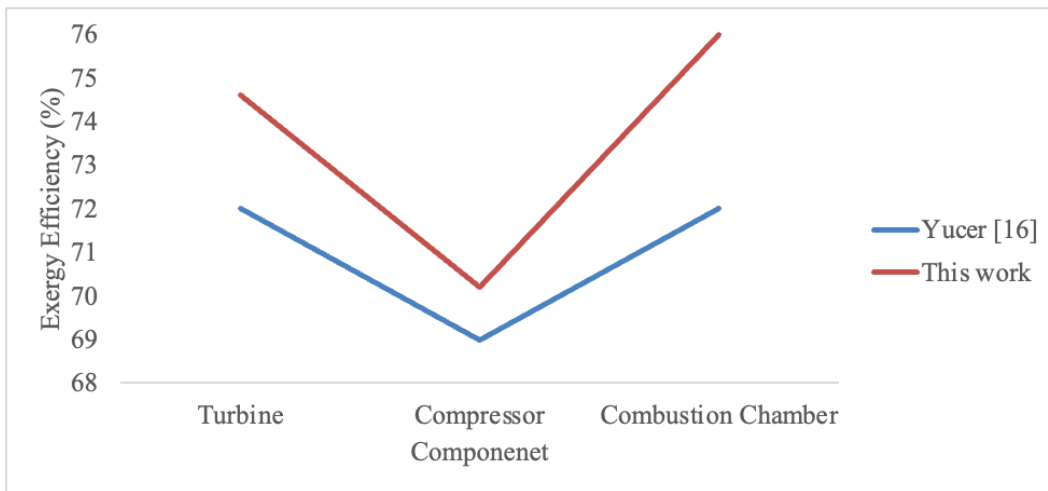


Figure 19. Validation of present work.

$$\eta_{II,component} = \frac{\text{Available exergy at output}}{\text{Available exergy at input}} \quad (10)$$

The configuration being considered for comparison is RGSASAC at 50% load condition for condenser pressure of 0.09 bar. The graph depicts the sametrend in the variationbut with higher values as described ahead. The higher values are obtained due to differing modelling considerations.

- The exergy efficiency of the turbine is high because of the reheat gas turbine with a closed-loop cooling of gas turbine blades while Yucer considers a simple jet engine.
- Compressor exergy efficiency is approximately the same as depicted in Figure 19.
- A higher value of exergy efficiency (approximately 4%) is obtained for the combustion chamber because of fuel preheating done by ammonia-water mixture. Fuel pre-heating decreases the fuel requirement for the same turbine inlet temperature, hence an increase in exergy efficiency of the combustion chamber.

CONCLUSION

Theparametric investigations on the part load operations of combined cycle arrangements having reheating in topping cycle and use of different cooling mediums for turbine entry temperature of 2000K & ambient temperature of 298Kyield the following major conclusions:

- For all the CCPP under considations the exergy efficiency is minimum when absorber pressure is 3.0 bar. The configuration RGSASC has theleast second law efficiency of23.55% at a 25% part-load.
- Theelectricity cost produced is maximum when theseparator temperature is 353K. The combined cycle configuration RGAAC has themaximum cost of electricity as 0.124USD/kWh, under this condition.

- The change in deaerator pressure and steam bleed fraction depicts the same graphical outcomes for exergy efficiency and electricity cost under all part load conditions.
- The minimum electricity cost of production is 0.05USD/kWh at 25% part load for CCPP having double pressure HRVG's at condenser pressure of 0.09 bar.
- The cost of exergy destruction is maximum at the combustion chamber as \$0.61, followed by the combination of HRVG, feed heater, and absorber as \$0.06.
- The present study analyses the part-load performance of reheat gas turbine-based combined power cycles. This study can be further extended by exploring the method(s) to reduce the cost of electricity under the part-load operation while keeping in the exergy losses minimum.

NOMENCLATURE

Notation	Detail (Unit)
AWT	Ammonia-water turbine
Ammonia	
-water mixture	Binary mixture
c	Specific cost
C	Compressor
\dot{C}	Cost rate associated with inlet and outlet exergy streams
CC/RCC	Combustion/Reheat combustion chamber
CCPP	Combined cycle power plant
CEP	Condensate extraction pump
Co	Condenser
CLC	Closed loop cooling
D	Distributor
D/a	Deaerator
\dot{E}	Rate of exergy production
FH	Feed heater

HA/IA/LA	Ammonia water turbine(s) at different pressure levels i.e., high or intermediate or low	RHE or R/h	steam cycle and reheat aqua ammonia cycle
HD/ ID/ LD	Drums operating at different pressure respectively i.e., high or intermediate or low	s	Refrigerant heat exchanger
HE	Heat exchanger	S	Entropy (kJ/kg K)
HRSG/ HRVG	Waste heat recovery heat exchanger for generating steam/binary vapor	SLE	Separator
HS/IS/LS	High/ Intermediate/Low-pressure steam turbine	TIT	Second law efficiency (%)
LHV	Lower heating value (kJ/kg)	T	Turbine inlet temperature (Kelvin)
LT/ HT/LGT/HGT	Topping cycle turbo machines	T _o	Temperature (Kelvin)
\dot{m}	Mass flow rate (kg/second)	Turbo machines	Dead state temperature (Kelvin)
M (1, 2...)	Mixer	USD	Gas turbines
FIX	Base load operational cost of power plant		Currency used in the United States of America
p/P	Pressure (bar)	W	Work transfer
P (1,2, 3...)	Pump	\dot{Z}	Total cost rate associated with capital investment and operation and maintenance cost
P _o	Dead state pressure (bar)	Subscripts	
Q _{in}	Heat input to separator (kJ/kg)	a	Air/ambient
RGSSC	Reheat type steam cooled topping cycle with steam bottoming cycle.	abs.	Absorber
RGAAC	Reheat type aqua ammonia cooled topping cycle with aqua ammonia bottoming cycle	amwt	Ammonia-water mixture turbine
RGSASC	Reheat type steam cooled topping cycle with steam and aqua ammonia bottoming cycle	b	blade
RGSAAC	Reheat type aqua ammonia cooled topping cycle with steam and aqua ammonia bottoming cycle	b/s	bleed steam
RGSASAC	Reheat type steam and aqua ammonia mixture cooled topping cycle with steam and aqua ammonia bottoming cycle	c	Compressor
RGRSASC	Reheat type steam cooled topping cycle with reheat steam and aqua ammonia bottoming cycle	cc/rcc	Combustion chamber/Reheat combustion chamber
RGRSAAC	Reheat type aqua ammonia mixture cooled topping cycle with reheat steam and aqua ammonia bottoming cycle	cw/w	Cooling water/water
RGRSASAC	Reheat type steam and aqua ammonia mixture cooled topping cycle with steam and aqua ammonia bottoming cycle	d/a	Deaerator
RGRSRASC	Reheat type steam cooled topping cycle with steam and reheat aqua ammonia bottoming cycle	f/fg	Fuel/flue gas
RGRSRAAC	Reheat type aqua ammonia mixture cooled topping cycle with reheat steam and aqua ammonia bottoming cycle	fc	High pressure fuel injector
RGRSASAC	Reheat type steam and aqua ammonia mixture cooled topping cycle with steam and aqua ammonia bottoming cycle	gen	Generator
RGRSRASC	Reheat type steam cooled topping cycle with steam and reheat aqua ammonia bottoming cycle	gt	Gas turbine
RGRSRAAC	Reheat type aqua ammonia mixture cooled topping cycle with reheat steam and aqua ammonia bottoming cycle	HE	Heat exchanger
RGRSASAC	Reheat type steam and aqua ammonia mixture cooled topping cycle with steam and aqua ammonia bottoming cycle	hp/ip/lp	High /Intermediate/Low pressure
RGRSRASC	Reheat type steam cooled topping cycle with steam and reheat aqua ammonia bottoming cycle	i	Inlet/initial
RGRSRAAC	Reheat type aqua ammonia mixture cooled topping cycle with reheat steam and aqua ammonia bottoming cycle	is	Isentropic
RGRSASAC	Reheat type steam and aqua ammonia mixture cooled topping cycle with steam and aqua ammonia bottoming cycle	M	Mechanical
RGRSRASC	Reheat type steam cooled topping cycle with steam and reheat aqua ammonia bottoming cycle	M/C	Mechanical chiller
RGRSRAAC	Reheat type aqua ammonia mixture cooled topping cycle with reheat steam and aqua ammonia bottoming cycle	o/e	Outlet/Exit
RGRSASAC	Reheat type steam and aqua ammonia mixture cooled topping cycle with steam and aqua ammonia bottoming cycle	q	Heat transfer
RGRSRASC	Reheat type steam cooled topping cycle with steam and reheat aqua ammonia bottoming cycle	ref.	Refrigerating effect
RGRSRAAC	Reheat type aqua ammonia mixture cooled topping cycle with reheat steam and aqua ammonia bottoming cycle	ri	Rich
RGRSASAC	Reheat type steam and aqua ammonia mixture cooled topping cycle with steam and aqua ammonia bottoming cycle	s/st	Steam
RGRSRASC	Reheat type steam cooled topping cycle with steam and reheat aqua ammonia bottoming cycle	sol.	Solution
RGRSRAAC	Reheat type aqua ammonia mixture cooled topping cycle with reheat steam and aqua ammonia bottoming cycle	we	Weak
RGRSASAC	Reheat type steam and aqua ammonia mixture cooled topping cycle with steam and aqua ammonia bottoming cycle	wo/w	Working
RGRSRASC	Reheat type steam cooled topping cycle with steam and reheat aqua ammonia bottoming cycle	Superscrip	
RGRSRAAC	Reheat type aqua ammonia mixture cooled topping cycle with reheat steam and aqua ammonia bottoming cycle	CI	Capital investment
RGRSASAC	Reheat type steam and aqua ammonia mixture cooled topping cycle with steam and aqua ammonia bottoming cycle	OM	Operation and maintenance
RGRSRASC	Reheat type steam cooled topping cycle with steam and reheat aqua ammonia bottoming cycle	Greek letters:	
RGRSRAAC	Reheat type aqua ammonia mixture cooled topping cycle with reheat steam and aqua ammonia bottoming cycle	ω	Variable used in economic analysis
RGRSASAC	Reheat type steam and aqua ammonia mixture cooled topping cycle with steam and aqua ammonia bottoming cycle	η	Efficiency
RGRSRASC	Reheat type steam cooled topping cycle with steam and reheat aqua ammonia bottoming cycle	α	Cost (USD)
RGRSRAAC	Reheat type aqua ammonia mixture cooled topping cycle with reheat steam and aqua ammonia bottoming cycle	γ	Variable used in economic analysis

AUTHORSHIP CONTRIBUTIONS

Authors equally contributed to this work.

DATA AVAILABILITY STATEMENT

The authors confirm that the data that supports the findings of this study are available within the article. Raw data that support the finding of this study are available from the corresponding author, upon reasonable request.

CONFLICT OF INTEREST

The author declared no potential conflicts of interest with respect to the research, authorship, and/or publication of this article.

ETHICS

There are no ethical issues with the publication of this manuscript.

REFERENCES

- [1] Tsatsaronis G, Winhold M. Exergoeconomic analysis and evaluation of energy-conversion plants-I. A new general methodology. *Energy* 1985;10:69–80. [\[CrossRef\]](#)
- [2] Abusoglu A, Kanoglu M. Exergoeconomic analysis and optimization of combined heat and power production: A review. *Renew Sustain Energy Rev* 2009;13:2295–2308. [\[CrossRef\]](#)
- [3] Tsatsaronis G. Exergoeconomics: Is it only a new name?. *Chem Eng Technol* 1996;19:163–169. [\[CrossRef\]](#)
- [4] Gorji-Bandpy M, Ebrahimian V. Exergoeconomic analysis of gas turbine power plants. *Int Energy J* 2006;7:57–67.
- [5] Tsatsaronis G, Lin L, Pisa J. Exergy costing in exergoeconomics. *J Energy Resour Technol* 1993;115:9–16. [\[CrossRef\]](#)
- [6] Zhang G, Hua B, Chen Q. Exergoeconomic methodology for analysis and optimization of process systems. *Comput Chem Eng* 2000;24:613–618. [\[CrossRef\]](#)
- [7] Ozdil NF, Tantekin A, Pekdur A. Thermodynamic, economic and environmental assessments in a cogeneration power plant. *Energy Sources Part A: Recov Util Environ Eff* 2020;42:149–169.
- [8] Balafkandeh S, Zare V, Gholamian E. Multi-objective optimization of a tri-generation system based on biomass gasification/digestion combined with S-CO₂ cycle and absorption chiller. *Energy Convers Manag* 2019;200:112057. [\[CrossRef\]](#)
- [9] Gholamian E, Habibollahzade A, Zare V. Development and multi-objective optimization of geothermal-based organic Rankine cycle integrated with thermoelectric generator and proton exchange membrane electrolyzer for power and hydrogen production. *Energy Convers Manag* 2018;174:112–125. [\[CrossRef\]](#)
- [10] Motamed MA, Nord LO. Assessment of organic rankine cycle part-load performance as gas turbine bottoming cycle with variable area nozzle turbine technology. *Energies* 2021;14:7916. [\[CrossRef\]](#)
- [11] Ozdil NFT, Pekdur A. Energy and exergy assessment of a cogeneration system in food industry: a case study. *Int J Exergy* 2016;20:254–268.
- [12] Ozdil NFT, Tantekin A. Exergoeconomic analysis of a FBCC steam power plant. *Therm Sci* 2017;21:1975–1984. [\[CrossRef\]](#)
- [13] Ozdil NF, Tantekin A, Pekdur A. Performance assessment of a cogeneration system in food industry. *J Therm Eng* 2018;4:1847–1854. [\[CrossRef\]](#)
- [14] Tantekin A, Ozdil NF. Thermodynamic analysis of a fluidized bed coal combustor steam plant in textile industry. *J Therm Eng* 2017;3:1607–1614. [\[CrossRef\]](#)
- [15] Fellah GM, Mghrebi FA, Aboghres SM. Exergoeconomic analysis for unit Gt14 of South Tripoli gas turbine power plant. *Jordan J Mech Ind Eng* 2010;4:507–516.
- [16] Yucer CT. Thermodynamic analysis of the part load performance for a small scale gas turbine jet engine by using exergy analysis method. *Energy* 2016;111:251–259. [\[CrossRef\]](#)
- [17] Li Y, Zhang G, Bai Z, Song X, Wang L, Yang Y. Backpressure adjustable gas turbine combined cycle: A method to improve part-load efficiency. *Energy Convers Manag* 2018;174:739–754. [\[CrossRef\]](#)
- [18] Liu T, Zhang G, Li Y, Yang Y. Performance analysis of partially recuperative gas turbine combined cycle under off-design conditions. *Energy Convers Manag* 2018;162:55–65. [\[CrossRef\]](#)
- [19] Bakhshmand SK, Saray RK, Bahlouli K, Eftekhari H, Ebrahimi A. Exergoeconomic analysis and optimization of a triple-pressure combined cycle plant using evolutionary algorithm. *Energy*. 2015;93:555–567. [\[CrossRef\]](#)
- [20] Sahin AZ, Al-Sharafi A, Yilbas BS, Khaliq A. Overall performance assessment of a combined cycle power plant: an exergo-economic analysis. *Energy Convers Manag* 2016;116:91–100. [\[CrossRef\]](#)
- [21] Ameri M, Ahmadi P, Hamidi A. Energy, exergy and exergoeconomic analysis of a steam power plant: A case study. *Int J Energy Res* 2009;33:499–512. [\[CrossRef\]](#)
- [22] Variny M, Mierka O. Improvement of part load efficiency of a combined cycle power plant provisioning ancillary services. *Appl Energy* 2009;86:888–894. [\[CrossRef\]](#)
- [23] Soltani S, Mahmoudi SMS, Yari M, Morosuk T, Rosen MA, Zare V. A comparative exergoeconomic analysis of two biomass and co-firing combined power plants. *Energy Convers Manag* 2013;76:83–91. [\[CrossRef\]](#)

- [24] Khanmohammadi S, Azimian AR. Exergoeconomic evaluation of a two-pressure level fired combined-cycle power plant. *J Energy Eng* 2015;141:04014014. [\[CrossRef\]](#)
- [25] Mehrpooya M, Taromi M, Ghorbani B. Thermo-economic assessment and retrofitting of an existing electrical power plant with solar energy under different operational modes and part load conditions. *Energy Rep* 2019;5:1137–1150. [\[CrossRef\]](#)
- [26] Najjar YS, Alalul OF, Abu-Shamleh A. Degradation analysis of a combined cycle heat recovery steam generator under full and part load conditions. *Sustain Energy Technol Assess*. 2020;37:100587. [\[CrossRef\]](#)
- [27] Jonshagen K. Exhaust Gas Recirculation to Improve Part Load Performance on Combined Cycle Power Plants. In: *ASME Turbo Expo 2016: Turbomachinery Technical Conference and Exposition*, 2016. p. V003T06A004. [\[CrossRef\]](#)
- [28] Maheshwari M, Singh O. Exergy analysis of inter-cooled reheat combined cycle with ammonia water mixture based bottoming cycle. *Appl Therm Eng* 2017;121:820–827. [\[CrossRef\]](#)
- [29] Song TW, Sohn JL, Kim JH, Kim TS, Ro ST. Exergy-based performance analysis of the heavy-duty gas turbine in part-load operating conditions. *Exergy Int J* 2002;2:105–112. [\[CrossRef\]](#)
- [30] Ganjehkaviri A, Jaafar MM, Ahmadi P, Barzegaravval H. Modelling and optimization of combined cycle power plant based on exergoeconomic and environmental analyses. *Appl Therm Eng* 2014;67:566–578. [\[CrossRef\]](#)
- [31] Liu Z, Karimi IA. Simulation and optimization of a combined cycle gas turbine power plant for part-load operation. *Chem Eng Res Des* 2018;131:29–40. [\[CrossRef\]](#)
- [32] Baghernejad A, Yaghoubi M. Exergoeconomic analysis and optimization of an Integrated Solar Combined Cycle System (ISCCS) using genetic algorithm. *Energy Convers Manag* 2011;52:2193–2203. [\[CrossRef\]](#)
- [33] Lorencin I, Anđelić N, Mrzljak V, Car Z. Genetic algorithm approach to design of multi-layer perceptron for combined cycle power plant electrical power output estimation. *Energies* 2019;12:4352. [\[CrossRef\]](#)
- [34] Dawo F, Wieland C, Spliethoff H. Kalina power plant part load modeling: Comparison of different approaches to model part load behavior and validation on real operating data. *Energy* 2019;174:625–637. [\[CrossRef\]](#)
- [35] Sanjay Y, Singh O, Prasad BN. Energy and exergy analysis of steam cooled reheat gas-steam combined cycle. *Appl Therm Eng* 2007;27:2779–2790. [\[CrossRef\]](#)
- [36] Zare V, Mahmoudi SMS. A thermodynamic comparison between organic Rankine and Kalina cycles for waste heat recovery from the Gas Turbine-Modular Helium Reactor. *Energy* 2015;79:398–406. [\[CrossRef\]](#)
- [37] Yari M, Mahmoudi SMS. Utilization of waste heat from GT-MHR for power generation in organic Rankine cycles. *Appl Therm Eng* 2010;30:366–375. [\[CrossRef\]](#)
- [38] Yari M, Mehr AS, Zare V, Mahmoudi SMS, Rosen MA. Exergoeconomic comparison of TLC (trilateral Rankine cycle), ORC (organic Rankine cycle) and Kalina cycle using a low grade heat source. *Energy* 2015;83:712–722. [\[CrossRef\]](#)
- [39] Bolz RE. *CRC Handbook of Tables for Applied Engineering Science*. Boca Raton, Florida: CRC Press; 1973.
- [40] Cengel YA, Boles MA. *Thermodynamics: An Engineering Approach*. New York: McGraw-Hill; 2002.
- [41] Maheshwari M, Singh O. Thermo-economic analysis of combined cycle configurations with intercooling and reheating. *Energy* 2020;25:118049. [\[CrossRef\]](#)
- [42] Prakash D, Singh O. Thermo-economic study of combined cycle power plant with carbon capture and methanation. *J Clean Product* 2019;231:529–542. [\[CrossRef\]](#)
- [43] Singh R, Singh O. Comparative study of combined solid oxide fuel cell-gas turbine-Organic Rankine cycle for different working fluid in bottoming cycle. *Energy Convers Manag* 2018;171:659–670. [\[CrossRef\]](#)
- [44] Owebor K, Oko COC, Diemuodeke EO, Ogorure OJ. Thermo-environmental and economic analysis of an integrated municipal waste-to-energy solid oxide fuel cell, gas-, steam-, organic fluid-and absorption refrigeration cycle thermal power plants. *Appl Energy* 2019;239:1385–1401. [\[CrossRef\]](#)
- [45] Campbell JM. *Gas Conditioning and Processing*, Vol. 1, the Basic Principals. 8th ed. Norman, Oklahoma: Campbell Petroleum Series; 2001.
- [46] Gulen SC. A more accurate way to calculate the cost of electricity. *Power* 2011;155:62–65.
- [47] Central Electricity Regulatory Commission New Delhi. *Tariff (Regulation) norms 2014*, order no. L-1/144/2013/CERC. Central Electricity Regulatory Commission New Delhi.